

**The impact of biodiesel from *Crambe tataria* and *Crambe orientalis* on engine
performance, combustion, and exhaust emissions**

Ayhan UYAROĞLU^{a,*}, İsmet ÇELİKTEN^b

^aCihanbeyli Vocational High School, Selçuk University, Konya, Turkey,
ayhan.uyaroglu@selcuk.edu.tr Orcid:<https://orcid.org/0000-0001-7914-9665>

^bEmeritus Professor (retired), Faculty of Technology, Gazi University, Ankara, Turkey,
ismetcelikten@hotmail.com

*Corresponding author: ayhan.uyaroglu@selcuk.edu.tr (Ayhan Uyaroglu)

Tel.: +905054250235

Abstract

Crambe tataria and *Crambe orientalis* are non-cultivated plant species in Türkiye that can survive under harsh natural conditions. Due to their erucic acid content, their oils are not considered edible. Biodiesel derived from non-edible oils offers a significant renewable fuel surrogate for internal combustion engine applications, providing favorable environmental and economic outcomes. The aim of the current experimental study is to explore and measure the effects of petroleum-based diesel fuel and fuel mixtures of *Crambe tataria* and *Crambe orientalis* oil methyl esters on the performance and emission characteristics of a single-cylinder, four-stroke, naturally aspirated, direct injection compression ignition (CI) engine. The arranged test fuel samples consisted of six different mixtures by volume: COB20, COB40, COB60, and CTB20, CTB40, CTB60. The standard diesel fuel was denoted as D0. Tests on the engine were carried out at load levels of 15 N, 30 N, 45 N, and 60 N, with the engine speed stabilized at 2200 rpm. Pursuant to the experimental results, the brake specific fuel consumption (BSFC), NO_x emission values, and combustion duration of the biodiesel mixture fuels were come by greater. HC, CO, and soot emissions, heat dissipation rates, in-cylinder temperature, cumulative

heat release rate, indicated mean effective pressure (IMEP), and rate of pressure rise (RI) values were detected in lesser match against to diesel fuel. As a result, the findings indicate that biodiesels from *Crambe tataria* and *Crambe orientalis* have the capability to replace petroleum-based diesel fuel in CI engine applications.

Keywords: *Crambe tataria*, *crambe orientalis*, biodiesel, combustion, emissions

1- Introduction

Internal combustion engines are machines that convert fuel energy into mechanical energy, thereby facilitating various aspects of human life. Internal combustion engines remain prevalent in the transportation industry, [1] with diesel engines being extensively utilized owing to their superior power output, thermal efficiency, and fuel consumption characteristics [2]. In this regard, compression-ignition (CI) engines are likely to remain in use for an extended period in heavy-duty vehicles operating across road transportation, public transit systems, and maritime logistics [3]. Fossil fuels continue to play a central role in global energy production, with widespread utilization in sectors such as transportation [4]. Nevertheless, the imperative for low-emission and high-efficiency propulsion technologies has accelerated the pursuit of sustainable alternatives [5]. Biodiesel, a renewable biofuel derived from biological feedstocks, is increasingly recognized as a promising substitute for petroleum-based diesel [6]. Its environmental advantages include the reduction of lifecycle greenhouse gas emissions, minimization of ecological degradation, and potential to contribute to energy security amidst the ongoing global energy crisis [7]. Thenceforth the discovery of internal combustion engines, efforts have continued to explore the use of various fuels to operate these engines. In the search for alternative fuels, fluctuations have occurred over time due to both the desire to reduce dependence on petroleum and growing environmental concerns. During periods of oil crises, research on alternative fuels intensified; however, interest declined once the crises were

overcome. In recent years, environmental factors have come to the forefront, leading to a renewed increase in such research efforts. Biodiesel's history as a diesel engine alternative stretches back to 1900, when its inventor, Rudolf Diesel, powered his engine with peanut oil during the Paris Exposition [8].

The increased demand for edible oils in biodiesel production has resulted in price hikes, elevating the cost of biodiesel and edible oils to 1.5–2 times that of diesel fuel. In biodiesel production costs, the largest share approximately 75–80% is attributed to the cost of the oil. Therefore, non-edible oils are gaining traction as attractive and sustainable feedstocks for biodiesel manufacturing [9]. Non-edible feedstocks represent a sustainable option for biofuel generation, as they are predominantly grown on waste or marginal lands, deliver yields that rival or exceed edible feedstocks, and are remarkably cost-efficient [10]. Biodiesel production from non-renewable biological sources not only reduces dependency on imports but also contributes to rural development. Through transesterification, biodiesel produced from such feedstocks offers a more effective solution for the "Blending Program" in developing countries, where the primary sector (agriculture) makes a significant help to Gross Domestic Product (GDP) [11].

Crambe tataria and *Crambe orientalis*, belonging to the Brassicaceae family, are perennial oilseed plants that grow naturally in Türkiye and are not cultivated. Due to their erucic acid content, they are classified as non-edible. Among the *Crambe* L. species, of which three species and five taxa are naturally procured in Türkiye, *Crambe tataria* Sebeok grows in Central Anatolia, and one of its taxa is endemic to southern Türkiye. *Crambe orientalis* L. is widely distributed across Central Anatolia, Eastern Anatolia, and Southeastern Anatolia. The plant height of *Crambe orientalis* ranges from 71 to 120 cm, while that of *Crambe tataria* ranges from

73 to 116 cm. The number of branches for *Crambe tataria* and *Crambe orientalis* has been determined to range through 2 to 15 and 1 to 10, in turn. The pod lengths of *Crambe orientalis* and *Crambe tataria* range through 2.9 to 5.22 mm and 2.81 to 4.21 mm, respectively, while the pod weight and thousand seed weight of *Crambe orientalis* range from 10.0 to 29.0 g and 7.0 to 14.60 g, in turn. For *Crambe tataria*, these values range through 9.0 to 18.0 g for pod weight and from 7.10 to 11.0 g for thousand seed weight. The dehulled oil content of *Crambe tataria* and *Crambe orientalis* seeds is 25% and 26%, respectively [12]. Erucic acid (C22:1, Δ -9, erucic acid) is a very long-chain monounsaturated fatty acid that serves as an significant oleochemical product due to its hydrophobicity and water resistance. It is extensively used across metallurgy, machinery, rubber, chemical industries, and many other fields [13]. The classification of erucic acid as a toxic substance stems from its involvement in Toxic Oil Syndrome and research suggesting cardiotoxicity in rats [14].

During engine experiments with B0, B5, B20, B50, and B100 fuels across four injection pressures (18, 20, 22, and 24 MPa) and indicated mean effective pressures values (12.5, 25, 37.5, and 50 kPa), biodiesel was found to raise BSFC, carbon dioxide, nitrogen oxides, and oxygen emissions, while lowering smoke opacity, unburned hydrocarbons, and carbon monoxide emissions. It has been reported that heightened injection pressure decreases brake specific fuel consumption (BSFC), smoke opacity, CO, and UHC emissions, while boosting CO₂, O₂ and NO_x emissions for high-percentage biodiesel–diesel mixtures such as B20, B50, and B100 [15].

Soybean oil biodiesel exhibited a BSFC that was 14.65% higher and smoke opacity up to 48.23% lower check against to diesel fuel. Additionally, CO emissions diminished by 11.36% with B20 and by 41.7% with B100, relative to diesel fuel. Entire soybean methyl ester (SME)

mixtures demonstrated a marked reduction in unburned hydrocarbon (UHC) emissions across the entire load range relative to diesel fuel. All SME mixtures exhibited elevated concentrations of NO_x pollutants during testing [16].

Aksoy et al. (2017) explored the performance of B30 fuel at 2200 rpm under five varying engine loads, evaluating aspects like in-cylinder pressure, heat release rate, cyclic alterations, combustion duration, and emissions including CO, CO₂, NO_x, and soot. They reported that, compared to diesel, B30 paved the way increased in-cylinder pressure and heat release rate under all engine loads due to improved oxidation reactions. At 18.75 Nm, CO and soot emissions were lessened by approximately 57.9% and 25.5%, respectively, check against to diesel. Additionally, B30 yielded higher indicated mean effective pressure (IMEP) and a shorter combustion duration [17].

Uyumaz (2018) tested mustard oil biodiesel–diesel fuel blends (M10, M20, M30) and standard diesel fuel (D100) at a peak brake torque speed of 2200 rpm, under four varying engine loads and full load conditions. At peak load, it was determined that, compared to D100, thermal efficiency diminished by 6.8% with M10, while BSFC raised by 4.8%. Confront with the diesel, the utilise of mustard oil biodiesel–diesel fuel mixtures resulted in significant downfalls in CO and smoke emissions, while an increment in NO_x emissions was observed with mustard oil biodiesel fuel blends. Additionally, it was denoted that there was no notable difference in cylinder pressure among mustard oil biodiesel–diesel fuel mixtures and diesel fuel [18].

Aksoy and Yılmaz (2019) operated the test engine at 2200 rpm, the speed of maximum torque, under four different engine loads. They investigated variations in cylinder pressure, heat release, combustion duration, ignition delay, indicated thermal efficiency, and specific fuel

consumption. Using fish oil biodiesel, they beheld an increment in cylinder pressure and heat release, along with a shortened combustion duration. However based upon the lesser calorific value of fish oil, a cutback in indicated mean effective pressure and indicated thermal efficiency was reported when using biodiesel. They reported that specific fuel consumption upsurged by approximately 32% with the B10 fuel blend [19].

In their study, Onukwuli et al. (2021) concluded that the combustion emission impacts of *Dyacrodes edulis* biodiesel blends, except for NO_x, were reduced confront with the petrodiesel. They found that brake thermal efficiency (BTE), BSFC, brake mean effective pressure (BMEP), volumetric efficiency, and exhaust temperature raised with brake power, while specific energies diminished with increasing load [20].

Reksowardojo et al. (2023) stated that the CO, HC, and particulate emissions of the B30, B50, and B100 fuels used in the experiment were lesser than those of diesel fuel, while NO_x emissions were heightened. With high-percentage biodiesel, they observed that the maximum power output decreased by up to 10% with B100. According to the modified carbon equilibrium formula for high-percentage biodiesel fuels, the fuel economy of B30, B50, and B100 biodiesels was procured to be 3%, 7%, and 11% smaller than that of diesel fuel, in turn [21].

Khalaf et al. (2024), in their study conducted with B20, B40, and B60 *Jatropha* and castor biodiesels under varying engine loads from no load to full load, reported that *Jatropha* biodiesel performed excelled performance and lesser emissions check against to castor biodiesel. They also found that the B20 blend delivered the superior performance and diminished emissions at all engine loads. They stated that, compared to conventional diesel, biodiesel sparked off lesser brake thermal efficiency (BTE), carbon monoxide (CO), carbon dioxide (CO₂), hydrocarbon

(HC), and smoke emissions, but led to elevated exhaust gas temperature (EGT), brake specific fuel consumption (BSFC), and nitrogen oxide (NO_x) emissions [22].

There were no reports on *C. orientalis* and *C. tataria* biodiesel combustion, performance and emissions. This study aims to assess the performance, combustion, and emission characteristics of biodiesel fuels (COB20, COB40, COB60 and CTB20, CTB40, CTB60), derived from *Crambe tataria* and *Crambe orientalis*—non-edible oil plants that are not cultivated in Türkiye and contain erucic acid—as alternative fuels in a diesel engine.

2. Material and methods

2.1 The engine test setup and specifications

In the test setup consisting of a single-cylinder diesel engine, dynamometer, emission analyser, smoke meter, precision balance, data acquisition card, thermocouples, and a computer, the emission, performance, and combustion characteristics of biodiesel fuels blended with standard diesel fuel at 20%, 40%, and 60% ratios were investigated at a stable engine speed of 2200 rpm under engine loads of 15 N, 30 N, 45 N, and 60 N. Additionally, a pressure sensor was used to measure in-cylinder pressure, and an encoder with a resolution of 0.36° crank angle (°CA) was exploited to measure the engine crank angle. In the engine tests, a Cussons P8160 model single-cylinder regenerative DC electric dynamometer was used. A schematic portrayal of the test set-up operated for the trials is presented in Figure 1.

Figure 1

Table 1 presents the technical characteristics of the single-cylinder Antor diesel engine occupied in the experiments.

Table 1

For the measurement of THC, CO, CO₂, and NO_x emissions, an EGAS-2M exhaust gas analyser manufactured by Environment SA was used, while soot emissions were measured using the AVL DiSmoke 4000 device. Table 2 screens the properties of these devices.

Table 2

The specifications of the AVL 8QP500c quartz pressure sensor used for measuring in-cylinder pressure numbers are served in Table 3.

Table 3

The specifications of the exhaust gas analyser and measurement devices are presented in Table 4. The parameters PU_{CO} , PU_{THC} , PU_{NOx} , PU_{Soot} , $PU_{Encoder}$, $PU_{Pressurebalance}$, and $PU_{Pressuresensor}$ represent the percentage uncertainty (PU) values associated with the measurements of CO, HC, NO_x, soot, precision balance, and pressure sensors, respectively. These PU values were calculated using Eq. (1), while the total uncertainty (TU) was determined based on Eq. (2) [23]. The overall TU value was computed to be 0.55%.

$$PU = \left(\frac{\text{Sensitivity or Accuracy}}{\text{Operating range}} \right) \times 100 \quad (1)$$

$$TU (\%) = \sqrt{(PU_{CO})^2 + (PU_{THC})^2 + (PU_{NOx})^2 + (PU_{Soot})^2 + (PU_{Encoder})^2 + (PU_{Pressuresensor})^2 + (PU_{Precisionbalance})^2} \quad (2)$$

Table 4

2.2 Combustion analysis measurement system and calculation method

In-cylinder pressure signals, captured over 50 engine cycles with a resolution of 2000 signals per cycle using the in-cylinder pressure sensor, were converted into pressure data via a data acquisition card and transferred to a computer. To enhance the accuracy and reliability of the test results, the average of 50 cycles was taken into account, and the evaluation was performed based on a single representative cycle.

Using the pressure data gathered as a function of crank angle for the fuels used in the experiments, variables such as in-cylinder gas temperature, combustion, heat release rate, indicated mean effective pressure (IMEP), maximum pressure rise rate (MPRR), combustion phases, combustion duration, rate of pressure rise (RI), and cyclic variations were reckoned in the MATLAB/Simulink environment.

Eq. (3), used to calculate the heat release rate as a function of crank angle, was derived from the First Law of Thermodynamics [24-25]. In Eq. (3), where heat transfer and gas leakage are neglected, θ symbolizes the crank angle, \dot{Q} depicts the heat release rate, P represents the in-cylinder pressure, V represents the cylinder volume, and k represents the isentropic index.

$$\frac{dQ}{d\theta} = \frac{k}{k-1} P \frac{dV}{d\theta} + \frac{1}{k-1} V \frac{dP}{d\theta} + \frac{dQ_{heat}}{d\theta} \quad (3)$$

Eq. (4) was used to calculate the indicated mean effective pressure (IMEP) [26-27].

$$I_{mep} = \frac{W_{net}}{V_{stroke}} \quad (4)$$

The cyclic differences of IMEP were calculated using Eq. (5) [23, 27-28].

$$COV_{imep} = \frac{\sigma_{imep}}{\bar{X}} \times 100 \quad (5)$$

Ringling intensity was determined using Eq. (6) [27-28].

$$RI = \frac{1}{2\gamma} \frac{\left(\beta \left(\frac{dP}{dt} \right)_{max} \right)^2}{P_{max}} \sqrt{\gamma \cdot R \cdot T_{max}} \quad (6)$$

2.3 Test Fuels

The *Crambe tataria* seeds used in the study were collected from the provinces of Karaman and Konya, while the *Crambe orientalis* seeds were gathered from the natural flora of Niğde. The oil from the collected seeds was extracted using a screw press at an oil processing facility located in the province of Konya. The properties of *Crambe tataria* and *Crambe orientalis* oils are presented in Table 5. Due to their erucic acid content approximately 37.11% in *Crambe tataria* and 44.32% in *Crambe orientalis* both are classified as non-edible oils. The production of biodiesel was achieved using a two-stage transesterification technique due to the oils being unrefined (crude) and the gelation issues encountered during preliminary trials. In the first stage of biodiesel generation through *crambe* oil, the crude oil was heated at 110 °C for 20 minutes to eliminate moisture and impurities. After reaching room temperature, 100 g of oil was taken and subjected to an esterification reaction with 1 g of sulphuric acid and 20 g of methanol at 50 °C for 1 hour at 600 rpm using a heated magnetic stirrer. At the end of the reaction, the blend

was transferred to a separation funnel and left for 2-3 hours for phase separation. The alcohol in the upper phase was removed, and the remaining oil in the lower phase was washed with a sodium bicarbonate solution at 85 °C to adjust the pH to 7. It was placed in a separation funnel and rested for a day. After the water remaining in the lower part was taken away, the oil was heated in a heated magnetic stirrer at 110 °C for 20 minutes to remove the water inside. Following these procedures, the oil was subjected to an optimization process in the second stage for the transesterification reaction using a basic catalyst. As a result of the optimization, for 100 g of oil, using 17 g of methanol and 0.42 g of NaOH at 57 °C for 1 hour, the yield (on a %w/w basis) was obtained as 97.1% for *Crambe tataria* and 96.5% for *Crambe orientalis*. The biodiesel–diesel blended fuels used in the experiments are as follows: For *C. tataria*: CTB20 (20% *C. tataria* + 80% diesel fuel), CTB40 (40% *C. tataria* + 60% diesel fuel), CTB60 (60% *C. tataria* + 40% diesel fuel); For *C. orientalis*: COB20 (20% *C. orientalis* + 80% diesel fuel), COB40 (40% *C. orientalis* + 60% diesel fuel), COB60 (60% *C. orientalis* + 40% diesel fuel); And for standard diesel fuel: D0. Table 6 presents some properties of the fuels deployed in the trials.

Table 5

Table 6

3. Result and discussion

3.1 Brake Fuel Specific Consumption

Figure 2 depicts the alteration of BSFC with respect to engine load. When examining the variations in specific fuel consumption of the fuels, it is monitored that the specific fuel consumption of biodiesel mixtures increases with the rising biodiesel percentage match against

to diesel fuel. The BSFC values of the biodiesel blended fuels COB20, COB40, COB60, CTB20, CTB40, and CTB60 increased by an average of 6.2%, 10.9%, 16.8%, 4.3%, 10.2%, and 14.5%, in turn, check against to diesel fuel. For this increase, Lapuerta et al. attested that on the occasion of the oxygen quantity of biodiesel fuel and its lesser calorific value, the brake specific fuel consumption (BSFC) is expected to increase by roughly 14% confront with diesel fuel [30]. In the same vein, Zhang et al. notified that the BSFC levels of biodiesel fuels increase by around 10%. This is attributed to their lesser calorific value and upward density. Since engine load increases, the impact of kinematic viscosity on BSFC can be fractionally reduced by reason of the rise in in-cylinder temperature [31]. Selvan et al. stated that further reason for the increase in SFC in mixtures is the variations in combustion phasing caused by the cetane number of biodiesel, along with the changes in injection timing [32].

Figure 2

3.2 Combustion Analysis

Figure 3 exhibits the alterations in in-cylinder pressure and heat release rate corresponding with crank angle. The in-cylinder pressure values of the fuels used in the trials increased with rising engine load. With increasing load, a subdued increase in the maximal in-cylinder pressures was observed over all fuels. This increment is attributed to the higher content of fuel injected into the cylinder, which in turn raises the in-cylinder temperature. In *Crambe tataria* and *Crambe orientalis* biodiesel blends, the pressure rise occurred earlier than in diesel fuel as the biodiesel proportion raised. This is on account of the earlier start of injection for biodiesel, which results from its elevated viscosity and density match against to diesel fuel, and besides lower compressibility of biodiesel relative to diesel fuel [33]. Additionally, the shorter ignition delay of biodiesel mixtured fuels sparks off an earlier start of combustion and consequently a prior

rise in pressure. The maximal pressure values of the biodiesel mixtured fuels were slightly lesser check against to those of diesel fuel. The variations in heat release can be observed in Figure 3. Heat release in compression ignition engines emanates in two stages: premixed combustion and diffusion combustion. In all biodiesel blends, combustion started earlier as the biodiesel ratio increased, and the heat release along the premixed combustion phase decreased with higher biodiesel content. The maximum heat dissipation rates of the biodiesel blended fuels COB20, COB40, COB60, CTB20, CTB40, and CTB60 were, on average, 17.1%, 23.6%, 24.9%, 9.9%, 24.9%, and 26.4% lesser, respectively, check against to diesel fuel. The elevated cetane number of biodiesel mixtures, and consequently their lessened ignition delay, along with their higher viscosity, surface tension, and poor spray atomization, contribute to the lower heat dissipation rate match against to diesel fuel [33-34]. Furthermore, the higher maximal heat dissipation rate of diesel fuel can be originated from its elevated calorific value confront with the biodiesel fuel blends.

Figure 3

Figure 4a shows the in-cylinder temperatures observed at a 60 N engine load. Based upon the smaller calorific number of biodiesel blended fuels, the in-cylinder gas temperatures were lesser match against to those of diesel fuel. The utmost in-cylinder temperature was obtained with diesel fuel at 1737.8 K, while the lowest was recorded with COB60 fuel at 1216.4 K. Figure 4b illustrates the alteration of cumulative heat dissipation corresponding with the crank angle at a 60 N engine load. The highest cumulative heat dissipation rate was recorded for diesel fuel at 2026.6 J/°CA, while the lowest was observed for COB60 fuel at 1685.8 J/°CA. For biodiesel blends, the cumulative heat release is lesser confront with the diesel fuel because of the fewer calorific number of the biodiesel blend [35].

Figure 4

Figure 5 illustrates the variations in CA10 and CA50. In internal combustion engines, the crank angle position related to 10% of the total heat release (CA10) is acceded to the start of combustion. The crank angle at which 50% of the cumulative heat dissipation ingenerates is referred to as CA50 [36]. CA50 is delayed as engine load increases, because with higher loads, the upsurged amount of fuel leads to a more pronounced diffusion combustion phase [37]. When examining CA10, it can be inferred that due to the high cetane number and consequently shorter ignition delay of biodiesel blended fuels, 10% of the heat release eventuates before top dead center (TDC). However, at a 60 N engine load, the increased quantity of fuel injected into the cylinder with rising load brings the effects of the elevated viscosity and density of biodiesel blended fuels to the forefront, redounding a delayed combustion match against to diesel fuel. When examining CA50, it can be stated that for each engine load, the CA50 levels of biodiesel blended fuels are superior compared to those of diesel fuel. This can be enunciated by matter of fact that biodiesel has the more density and viscosity than diesel, requiring the more time to complete the combustion process.

Figure 5

Declared as the range from start of combustion (SOC) to the end of combustion (EOC), combustion duration represents the total time needed for the complete combustion of the fuel. From the figure, it can be observed that diesel has a shorter combustion duration across all loads, whereas biodiesel blended fuels exhibit longer combustion durations. Additionally, as the load increases, combustion duration tends to increase for all fuel blends. This increase in combustion duration for the biodiesel blended fuels COB20, COB40, COB60, CTB20, CTB40,

and CTB60 was determined to be, on average, 26.6%, 25.1%, 21.4%, 17.5%, 28.5%, and 28.7% upper than that of diesel fuel, respectively. At low engine loads, the more combustion duration of biodiesel can be redounded to its logy evaporation characteristics due to lower fuel injection quality and larger droplet sizes. A longer diffusion combustion stage also leads to more combustion duration in all ester fuels match against to diesel [35]. The elevated kinematic viscosity of biodiesel is believed to significantly hinder the fuel spray, evaporation, and atomization processes, begetting in slower combustion and thus longer combustion duration [38-39]. Additionally, the longer ignition delay of diesel fuel enables more fuel to piling up in the cylinder, enabling superior air–fuel mixing and thereby improving combustion.

Figure 6

RI (ringing intensity) variations are presented in Figure 7. The maximum pressure rise rate, which varies depending on factors such as engine speed, is an indicator of the engine's knock tendency [40]. High ringing intensity (RI) leads to excessive combustion noise and can cause damage to engine components [33]. It was behelded that the adding of biodiesel to diesel fuel reduced the RI. This reduction in RI for COB20, COB40, COB60, CTB20, CTB40, and CTB60 biodiesel blended fuels was determined to be, on average, 22.8%, 33.6%, 45.2%, 17.7%, 43.1%, and 39.3% lower than that of diesel fuel, respectively. The lesser calorific value of biodiesel contributes to more stable combustion, resulting in lower RI values for biodiesel mixtures. Comparing to diesel fuel, biodiesel fuels are apt to produce lower vibration and noise levels [33]. Additionally, the oxygen quantity in biodiesel ameliorates combustion, which is also considered a contributing factor to the lessened RI values match against to diesel fuel.

Figure 7

The COV_{imep} value, which should not surpass 10% for stability of combustion and operation of internal combustion engines [19, 41], may vary from cycle to cycle due to factors such as leakage from piston rings, the valve system, or the cylinder head gasket, as well as residual exhaust gases remaining in the cylinder at the end of the exhaust stroke, all of which affect in-cylinder pressure and temperature [19]. Maximum cyclic differences are typically observed at the lowest engine load but tend to decrease as engine load spikes. The increased fuel delivery into the cylinder at higher loads pave the way in higher in-cylinder gas temperatures, improving combustion conditions and reducing cycle-to-cycle variations. Since the more viscosity and density of biodiesel blended fuels, fuel atomization deteriorates, coming to relatively elevated COV_{imep} values compared to diesel fuel.

Indicated mean effective pressure (IMEP), which is one of the key engine performance parameters, represents the average of the varying pressures exerted on the piston throughout a cycle. The figure displays the alterations in indicated mean effective pressure (IMEP) at a 60 N engine load over 50 cycles. On account of the elevated calorific value of diesel fuel confront with biodiesel blended fuels, higher IMEP values were observed for diesel. Another possible reason for the lower IMEP values of biodiesel blended fuels is their higher flash point relative to diesel fuel. This may weaken fuel evaporation and lead to the formation of heterogeneous pockets containing unevaporated liquid fuel when blended fuels are used. In addition, the higher viscosity of biofuels may further contribute to poor fuel blending and evaporation. It has been stated that higher-viscosity fuels can diminish in-cylinder efficiency, which may result in low engine performance fruitages for instance power, torque, and fuel efficiency [42].

Figure 8

3.3 Pollutant Emissions

Since hydrocarbon fuels burn in the cylinder of internal combustion engines at various air–fuel mixture ratios, they emit not only complete combustion products but also harmful emissions. These emissions are legally regulated. Furthermore, both engine design and fuel-related studies are ongoing to reduce them. Depending on fuel quality and blending ratio, the downfall in pollutant emissions can reach up to 78% [43].

CO emissions in compression ignition (CI) engines are significantly lower than those in gasoline engines due to the lean combustion conditions [44]. However, in diesel engines, the formation of CO emissions is attributed to partial or incomplete combustion, which results from heterogeneous mixture ratios, low in-cylinder pressure, oxygen deficiency, and lower charge mixture temperatures [34, 44-47]. Figure 9 shows the variations in CO emissions. The CO emission values of COB20, COB40, COB60, CTB20, CTB40, and CTB60 biodiesel blended fuels were, on average, reduced by 30.6%, 33.2%, 32.0%, 15.2%, 13.2%, and 11.7%, in turn, equiparated to diesel fuel. CO emissions upsurged for all fuels with increasing load. This increase is ascribed to the enrichment of the mixture due to greater fuel injection into the cylinder, which reduces oxidation reactions. Whenas biodiesel fuel is used in diesel engines, the reduction in CO emissions match against to diesel fuel has been connected with the oxygen quantity of biodiesel [34] and its elevated cetane number [44].

Unlike atmospheric oxygen, fuel-bound oxygen promotes combustion within fuel-rich spray patterns [44], and by mitigating the drop in post-combustion temperature, it facilitates the completion of oxidation reactions, thereby reducing CO emissions [46].

HC emissions, which originate from completely or partially unburned fuel, are primarily caused by poor fuel–air mixing and are not significantly affected by the overall air–fuel equivalence

ratio [48]. In addition, factors for instance high fuel evaporation heat, poor air–fuel mixture proportions, less flame speed, great fuel viscosity, and meagre atomization are among the key parameters contributing to unburned hydrocarbon (UHC) formation in the exhaust [45]. Figure 9 presents the fluctuation of HC emissions with relative to engine load. Equiparated to diesel fuel, the HC emissions of COB20, COB40, COB60, CTB20, CTB40, and CTB60 biodiesel blended fuels were, on average, reduced by 26.8%, 36.7%, 42.3%, 19.8%, 19.4%, and 24.1%, respectively. As engine load upswings, the quantity of fuel injected into the cylinder also raises, begetting to a rise in HC emissions over all fuel types. However, biodiesel fuel mixtures emitted lower HC emissions confront with the diesel fuel. This downfall is leaned on the more full combustion of the fuel, resulting from the higher molecular oxygen substance and great cetane number of biodiesel [22, 34, 47, 49].

Figure 9

NO_x emissions are subject to regulations to ensure they meet minimum standards, as they generate to the greenhouse effect, respiratory diseases, and a range of environmental concerns [50]. Possible factors for the increment in NO_x emissions in biodiesel fuels: Thermal NO_x formation, prompt NO_x formation, and fuel-bound nitrogen mechanisms [44]. Thermal NO_x formation appertains to cylinder temperature, oxygen level, and abode time [51]. Additionally, the amount of NO_x emissions spikes in direct proportion to the temperature of the engine's cylinder walls. Several factors, such as piston bowl geometry, extreme inlet air temperature, injection timing, and injection pressure, influence NO_x occurrence within the cylinder [47]. In addition, NO_x emissions are significantly affected by ignition delay [49]. A shorter ignition delay leads to a shorter mixing time, resulting in a slower combustion rate and a more gradual rise in pressure and temperature [34]. Kocakulak et al. 2023, has been reported that the addition

of carbon nanotubes (CNTs) significantly shorten ignition delay and enhance combustion dynamics in diesel engine systems. [52].

Possible factors for the increment in NO_x emissions in biodiesel fuels

- The higher the density, the higher the NO_x emissions tend to be, and vice versa. This is because the mass of fuel per unit volume inside the engine cylinder increases.
- Great fuel viscosity raises NO_x emissions. Higher fuel viscosity paves the way to an increment in mass injection. Fuel atomization percentages will decrease, leading to fuel impingement.
- A higher fuel bulk modulus results in increased NO_x emissions. Based upon the advanced injection and consequently elevated NO_x emissions, high-temperature conditions persist for a longer duration.
- Great surface tension sparks off the increased NO_x emissions. It has been noted that the surface tension of biodiesel is 22% superior than that of fossil diesel.
- A superior iodine value leads to increased NO_x emissions. Biodiesel with an iodine number lower than 40 is supposed to generate less NO_x.
- Methyl esters, characterized by two oxygen atoms per molecule, have a major impact on the iodine value. As mentioned earlier, the oxygen quantity primary affects NO_x emissions. Biodiesel's higher LHV (lower heating value) leads to elevated fuel consumption proportions and consequently elevated NO_x emissions. However, in some instances, incomplete combustion behavior results in lesser NO_x emissions, as stated in the literature [53].

Figure 10 shows the NO_x emissions of the test fuels. The CTB60 fuel performed the utmost NO_x values across all loads, with the highest increase of 24.8% observed at the 60N engine load. The increase in NO_x emissions for biodiesel mixture fuels is supported by the fact that biodiesel contains oxygen, has a longer combustion duration, and has higher viscosity and density.

Smoke emissions pose serious risks to both human health and the environment. They can cause headaches, chronic respiratory issues, allergic diseases, cancer, and growth retardation in infants. In compression ignition engines, smoke emissions are typically formed in regions of excessively rich combustion and uneven air–fuel mixtures [54]. Additionally, the sole visible exhaust gas, smoke opacity, is caused by the ingeneration of large fuel particles in areas with fuel-rich areas inside the combustion chamber, resulting in the presence of unburned fuel particles in the exhaust gases [55]. Both diesel and biodiesel fuels show an increase in smoke emissions as engine load increases. At same engine loads, diesel fuel generates more smoke emissions than alternative fuels. The soot emission graph is presented in Figure 10. Compared to diesel fuel, COB20, COB40, COB60, CTB20, CTB40, and CTB60 fuels have, on average, 9.1%, 17%, 26.2%, 6.1%, 13%, and 20.8% lower soot emissions, respectively. The lower soot emissions from biodiesel blended fuels are attributed to the oxygen substance and less sulphur quantity of biodiesel [56]. Additionally, the scarcity of aromatic compounds in biodiesel fuels, the lesser C:H ratio, and the surplus of O₂ molecules in fuel-rich pockets could increase engine combustion and fuel oxidation [57]. The less sulphur quantity of biodiesel, the entity of oxygen in its molecular structure, and great air excess ratios enhance combustion efficiency. While the minimal SO₃ emissions contribute to reducing smoke emissions [56], the oxygen component of biodiesel increases diffusion combustion, leading to more thorough oxidation of the produced particles. This makes biodiesel more effective in reducing smoke emissions [49].

Figure 10

Conclusion

The specific fuel consumption values of the fuels derived from *Crambe tataria* and *Crambe orientalis* biodiesel mixtures were attained to be higher at all engine loads match against to diesel fuel, based upon the relatively high viscosity, high density, and small calorific value of the biodiesel blends. The COB60 fuel showed the highest increase, with an average of 16.8%.

The heat release rates of all fuels initially increased with load but decreased at a 0.48 MPa load. This upward trend is due to the greater volume of fuel injected as the load increases, which results in warmer cylinder walls and elevated in-cylinder gas temperatures. However, at the 0.48 MPa load, despite the increased fuel amount, heat release decreased. This reduction is due to the enrichment of the fuel-air mixture and consequently worsened combustion. The notable increment in THC emissions at this load supports this reasoning. The least heat dissipation rate was observed with CTB60 fuel, at an average of 26.4%. Whereas the small calorific value of biodiesel blended fuels, the in-cylinder temperature and cumulative heat dissipation values are lesser check against to diesel fuel. Based upon the elevated viscosity and density of biodiesel fuels, the combustion duration is longer than that of diesel fuel, while the IMEP values are lower. With its inherent oxygen substance of biodiesel's, the RI numbers were found to be the lowest with COB60 fuel, at an average of 45.2%.

Across all engine loads, the fuels derived from *Crambe tataria* and *Crambe orientalis* biodiesel mixtures indicated lesser CO, CO₂, THC, and soot emission values match against to diesel fuel. However, NO_x emissions were found to be little higher compared to diesel fuel. As the biodiesel ratio raised in the biodiesel blends, emission values decreased. Overall, biodiesel blends have lower CO, CO₂, THC, and soot emissions. Nevertheless, by virtue of the risen volume of fuel injected into the cylinder with rising load, there was an increase in emission values for all fuels. On average, the greatest downfall was observed in CO emissions with

COB40 fuel (33.2%), in HC emissions with COB60 fuel (42.3%), and in soot emissions with COB60 fuel (26.2%). However, the highest increase in emissions occurred with CTB60 fuel at 60N engine load, with a 24.8% rise. *Crambe tataria* and *Crambe orientalis*, both non-edible oilseed plants, exhibit promising potential as alternative sources for biodiesel production. Notably, *Crambe orientalis* demonstrates superior fuel characteristics, including a higher calorific value and cetane number, alongside reduced emission levels compared to *Crambe tataria*.

The following topics are suggested for future studies:

- Visualisation and analysis of combustion flames
- Investigation of droplet size distribution in fuel injection systems
- Research into the effect of nano-based additives on fuel performance
- Assessment of the compatibility of two-stroke engines with alternative fuels

Acknowledgment

This study was supported Scientific Research Project Commission of Gazi University under Grant 07/2011-54. This article is produced from Ph.D. thesis of Ayhan UYAROĞLU.

References

1. Ardebili, S.M.S., Calam, A., Solmaz, H., et al. "Improving the combustion process of a homogeneous charge compression ignition engine running with triple fuel blend using response surface methodology", *J Braz. Soc. Mech. Sci. Eng.*, 46, 486 (2024). <https://doi.org/10.1007/s40430-024-05060-0>
2. Mahla, S.K., Ardebili, S.M.S., Rabeti, M., et al. "Performance and exhaust emissions analysis of a diesel engine running on diesel /diethyl ether/biogas as a green fuel", *Energy Sources, Part A: Recovery, Utilization, and Environmental Effects*, 44(4), pp. 9395–9411 (2022). <https://doi.org/10.1080/15567036.2022.2133194>
3. Solmaz, H., Calam, A., Yilmaz, E., et al. "Evaluation of MWCNT as fuel additive to diesel–biodiesel blend in a direct injection diesel engine", *Biofuels*, 14(2), pp. 147–156 (2022). <https://doi.org/10.1080/17597269.2022.2122154>
4. Polat, S., Calam, A., Ardebili, S.M.S., et al. "Operating Range, Performance and Emissions of an HCCI Engine Fueled with Fusel Oil/Diethyl Ether: An Experimental Study", *Sustainability*, 14(23), 15666 (2022). <https://doi.org/10.3390/su142315666>

5. Babagiray, M., Kocakulak, T., Ardebili, S.M.S. et al. "Optimization of operating conditions in a homogeneous charge compression ignition engine with variable compression ratio", *Int. J. Environ. Sci. Technol.*, 20, pp. 5311–5332 (2023). <https://doi.org/10.1007/s13762-022-04499-9>
6. Eslami, M.J., Hosseinzadeh Samani, B., Rostami, S., et al. "Investigating and optimizing the mixture of hydrogen-biodiesel and nano-additive on emissions of the engine equipped with exhaust gas recirculation", *Biofuels*, 14(5), pp. 473–484 (2023). <https://doi.org/10.1080/17597269.2022.2148877>
7. Shirneshan, A., Kanberoglu, B., Gonca, G., "Experimental investigation and parametric modeling of the effect of alcohol addition on the performance and emissions characteristics of a diesel engine fueled with biodiesel-diesel-hydrogen fuel mixtures", *Fuel*, 381, 133489 (2025). <https://doi.org/10.1016/j.fuel.2024.133489>
8. Pimentel, D., and Patzek, T.W., "Biofuels, solar and wind as renewable energy systems. Benefits and risks", pp. 157, New York: Springer, (2008). ISBN: 978-1-4020-8653-3
9. Chuah, L.F., Yusup, S., Aziz, A.R.A., et al. "Influence of fatty acids content in non-edible oil for biodiesel properties", *Clean Technologies and Environmental Policy*, 18, pp. 473–482 (2016). <https://doi.org/10.1007/s10098-015-1022-x>
10. Devarajan, Y., Munuswamy, D.B., Subbiah, G., et al. "Inedible oil feedstocks for biodiesel production: A review of production technologies and physicochemical properties", *Sustainable Chemistry and Pharmacy*, 30, 100840 (2022). <https://doi.org/10.1016/j.scp.2022.100840>
11. Kumar, A., Singh, V.P., Srivastava, A. "Quality biodiesel via biotransesterification from inedible renewable sources", *Journal of Cleaner Production*, 379, 134653 (2022). <https://doi.org/10.1016/j.jclepro.2022.134653>
12. Comlekcioglu, N., Karaman, S., Ilcim, A. "Oil composition and some morphological characters of *Crambe orientalis* var. *orientalis* and *Crambe tataria* var. *tataria* from Turkey", *Natural product research*, 22(6), pp. 525–532 (2008). <https://doi.org/10.1080/14786410701592349>
13. Wang P., Xiong X., Zhang X., et al. "A Review of Erucic Acid Production in Brassicaceae Oilseeds: Progress and Prospects for the Genetic Engineering of High and Low-Erucic Acid Rapeseeds (*Brassica napus*)", *Front. Plant Sci.*, 13:899076 (2022). doi: [10.3389/fpls.2022.899076](https://doi.org/10.3389/fpls.2022.899076)
14. Galanty, A., Grudzińska, M., Paździora, W., et al. "Erucic Acid—Both Sides of the Story: A Concise Review on Its Beneficial and Toxic Properties", *Molecules*, 28(4), 1924 (2023). <https://doi.org/10.3390/molecules28041924>
15. Gumus, M., Sayin, C., Canakci, M. "The impact of fuel injection pressure on the exhaust emissions of a direct injection diesel engine fueled with biodiesel–diesel fuel blends", *Fuel*, 95, pp. 486–494 (2012). <https://doi.org/10.1016/j.fuel.2011.11.020>
16. Al Dawody, M.F. and Bhatti, S.K. "Experimental and computational investigations for combustion, performance and emission parameters of a diesel engine fueled with soybean biodiesel-diesel blends", *Energy procedia*, 52, pp. 421–430 (2014). <https://doi.org/10.1016/j.egypro.2014.07.094>
17. Aksoy, F., Uyumaz, A., Boz, F., et al. "Experimental investigation of neutralized waste cooking oil biodiesel/diesel mixture and diesel fuel in a diesel engine at different engine loads", *International Journal of Automotive Science and Technology*, 1(1), pp. 7–15 (2017).
18. Uyumaz, A. "Combustion, performance and emission characteristics of a DI diesel engine fueled with mustard oil biodiesel fuel blends at different engine loads", *Fuel*, 212, pp. 256–267 (2018). <https://dx.doi.org/10.1016/j.fuel.2017.09.005>
19. Aksoy, F. and Yilmaz, E. "An Investigation of Combustion and Performance Characteristics of a Direct Injection Diesel Engine Fuelled With The Blends of 10% Fish

- Oil Biodiesel and 90% Diesel Fuel”, Gazi University Journal of Science Part C: Design and Technology, 7(1), pp. 12-24 (2019). DOI: [10.29109/gujsc.466544](https://doi.org/10.29109/gujsc.466544)
20. Onukwuli, O.D., Esonye C., Ofoefule A.U. “Combustion exhaust release impact, diesel engine performance, and optimization studies of green diesel-petrodiesel blend in a high compression ratio direct-injection compression-ignition engine”, *Advances in Mechanical Engineering*, 13(5), (2021). <https://doi.org/10.1177/16878140211018778>
 21. Reksowardojo, I.K., Setiaprada, H., Mokhtar, et al. “A study on utilization of high-ratio biodiesel and pure biodiesel in advanced vehicle technologies”, *Energies*, 16(2), 718 (2023). <https://doi.org/10.3390/en16020718>
 22. Khalaf, M., Xuan, T., Abdel-Fadeel, W.A., et al. “A comparative study of diesel engine fueled by Jatropa and Castor biodiesel: Performance, emissions, and sustainability assessment”, *Process Safety and Environmental Protection*, 188, pp. 453-466 (2024). <https://doi.org/10.1016/j.psep.2024.05.137>
 23. Uyumaz, A., Aksoy, F., Solmaz, H., et al. “Influences of carbon quantum dots nanoparticle addition to diesel-microwave-assisted corn oil biodiesel-dimethyl carbonate fuel blends on combustion, performance and emissions”, *Fuel*, 383, 133855 (2025). <https://doi.org/10.1016/j.fuel.2024.133855>
 24. Ferrari G, Onorati A, & D'Errico G. “Internal combustion engines”, pp. 506 Società Editrice 884 Esculapio; 2022.
 25. Heywood JB. “Internal combustion engine Fundamentals”, pp. 510 McGraw-Hill, Inc.; 1988.
 26. Yılmaz, E. “Investigation of the effects of diesel-fusel oil fuel blends on combustion, engine performance and exhaust emissions in a single cylinder compression ignition engine”, *Fuel*, 255, 115741 (2019). <https://doi.org/10.1016/j.fuel.2019.115741>
 27. Günaydin, S., Uyumaz, A., Kocakulak, T., et al. “Evaluation of dibutyl maleate/diesel blends on combustion, performance and emissions in a DI diesel engine”, *Applied Thermal Engineering*, 236, 121520 (2024). <https://doi.org/10.1016/j.applthermaleng.2023.121520>
 28. Uyumaz, A., Aksoy, F., Solmaz, H., et al. “Combustion, performance and emission evaluation of a diesel engine running on microwave-assisted corn oil biodiesel mixture with carbon quantum dot nanoparticle additive”, *International Journal of Hydrogen Energy*, 95, pp. 849-859 (2024). <https://doi.org/10.1016/j.ijhydene.2024.11.294>
 29. Can, Ö., Öztürk, E., Solmaz, H., et al. “Combined effects of soybean biodiesel fuel addition and EGR application on the combustion and exhaust emissions in a diesel engine”, *Applied thermal engineering*, 95, pp. 115-124 (2016). <http://dx.doi.org/10.1016/j.applthermaleng.2015.11.056>
 30. Lapuerta, M., Armas, O., Rodriguez-Fernandez, J. “Effect of biodiesel fuels on diesel engine emissions”, *Progress in energy and combustion science*, 34(2), pp. 198-223 (2008). <https://doi.org/10.1016/j.pecs.2007.07.001>
 31. Zhang, Z., Jiaqiang, E., Deng, Y., et al. “Effects of fatty acid methyl esters proportion on combustion and emission characteristics of a biodiesel fueled marine diesel engine”, *Energy Conversion and Management*, 159, pp. 244-253 (2018). <https://doi.org/10.1016/j.enconman.2017.12.098>
 32. Selvan, B.K., Das, S., Chandrasekar, M., et al. “Utilization of biodiesel blended fuel in a diesel engine–Combustion engine performance and emission characteristics study”, *Fuel*, 311, 122621 (2022). <https://doi.org/10.1016/j.fuel.2021.122621>
 33. Erdoğan, S., Balki, M.K., Sayin, C. “The effect on the knock intensity of high viscosity biodiesel use in a DI diesel engine”, *Fuel*, 253, pp. 1162-1167 (2019). <https://doi.org/10.1016/j.fuel.2019.05.114>

34. Ashok, B., Nanthagopal, K., Vignesh, D.S. "Calophyllum inophyllum methyl ester biodiesel blend as an alternate fuel for diesel engine applications", Alexandria engineering journal, 57(3), pp. 1239-1247 (2018). <https://doi.org/10.1016/j.aej.2017.03.042>
35. Rajasekar, E. And Selvi, S. "Review of combustion characteristics of CI engines fueled with biodiesel", Renewable and Sustainable Energy Reviews, 35, pp. 390-399 (2014). <https://doi.org/10.1016/j.rser.2014.04.006>
36. Calam, A. and Aydoğan, B. "Experimental investigation of performance combustion and emission characteristics in an HCCI engine fuelled isopropanol and heptane fuel mixtures", Gazi Üniversitesi Fen Bilimleri Dergisi Part C, 7(4), pp. 818-833 (2019). DOI:10.29109/gujsc.605057
37. Liu, H., Ma, X., Li, B., et al. "Combustion and emission characteristics of a direct injection diesel engine fueled with biodiesel and PODE/biodiesel fuel blends", Fuel, 209, pp. 62-68 (2017). <https://doi.org/10.1016/j.fuel.2017.07.066>
38. An, H., Yang, W.M., Maghbouli, A., et al. "Performance, combustion and emission characteristics of biodiesel derived from waste cooking oils", Applied energy, 112, pp. 493-499 (2013). <https://doi.org/10.1016/j.apenergy.2012.12.044>
39. Agarwal, A.K. and Dhar, A. "Experimental investigations of performance, emission and combustion characteristics of Karanja oil blends fuelled DIC engine", Renewable energy, 52, pp. 283-291 (2013). <https://doi.org/10.1016/j.renene.2012.10.015>
40. Opuz, M., Uyumaz, A., Babagiray, M., et al. "The effects of metallic fuel addition into canola oil biodiesel on combustion, engine performance and exhaust emissions", Journal of the Energy Institute, 111, 101390 (2023). <https://doi.org/10.1016/j.joei.2023.101390>
41. Çelik, M., Solmaz, H., Yücesu, H.S. "Examination of the effects of organic based manganese fuel additive on combustion and engine performance", Fuel Processing Technology, 139, pp. 100-107 (2015). <https://doi.org/10.1016/j.fuproc.2015.08.002>
42. Lodi, F., Zare, A., Arora, P., et al. "Engine performance characteristics using microalgae derived dioctyl phthalate biofuel during cold, preheated and hot engine operation", Fuel, 344, 128162 (2023). <https://doi.org/10.1016/j.fuel.2023.128162>
43. Stančin, H., Mikulčić, H., Wang, X., et al. "A review on alternative fuels in future energy system", Renewable and sustainable energy reviews, 128, 109927 (2020). <https://doi.org/10.1016/j.rser.2020.109927>
44. Hassan, T., Rahman, M.M., Adib, A.R., et al. "Effect of Ni and Al nanoadditives on the performance and emission characteristics of a diesel engine fueled with diesel-castor oil biodiesel-n-butanol blends", Case Studies in Chemical and Environmental Engineering, 8, 100531 (2023). <https://doi.org/10.1016/j.cscee.2023.100531>
45. Kalyani, T., Prasad, L.S.V., Kolakoti, A. "Effect of triacetin as an oxygenated additive in algae biodiesel fuelled CI engine combustion, performance, and exhaust emission analysis", Fuel, 338, 127366 (2023). <https://doi.org/10.1016/j.fuel.2022.127366>
46. Solmaz, H., Calam, A., Yilmaz, E., et al. "Evaluation of MWCNT as fuel additive to diesel-biodiesel blend in a direct injection diesel engine", Biofuels, 14(2), pp. 147-156 (2023). <https://doi.org/10.1080/17597269.2022.2122154>
47. Nayak, S.K., Hoang, A.T., Nayak, B., et al. "Influence of fish oil and waste cooking oil as post mixed binary biodiesel blends on performance improvement and emission reduction in diesel engine", Fuel, 289, 119948 (2021). <https://doi.org/10.1016/j.fuel.2020.119948>
48. Sayin, C. "DIESEL ENGINE EMISSIONS IMPROVEMENTS BY THE USE OF SUN FLOWER METHYL ESTER/DIESEL BLENDS", Journal of Thermal Science & Technology/Isı Bilimi ve Tekniği Dergisi, 33(2) (2013).
49. El-Shafay, A.S., Ağbulut, Ü., Attia, E.A., et al. "Waste to energy: Production of poultry-based fat biodiesel and experimental assessment of its usability on engine behaviors", Energy, 262, 125457 (2023). <https://doi.org/10.1016/j.energy.2022.125457>

50. Malik, M.A.I., Zeeshan, S., Khubaib, M., et al. "A review of major trends, opportunities, and technical challenges in biodiesel production from waste sources", *Energy Conversion and Management*: X, 100675 (2024). <https://doi.org/10.1016/j.ecmx.2024.100675>
51. Gad, M.S., El-Shafay, A.S., Hashish, H.A. "Assessment of diesel engine performance, emissions and combustion characteristics burning biodiesel blends from jatropha seeds", *Process Safety and Environmental Protection*, 147, pp. 518-526 (2021). <https://doi.org/10.1016/j.psep.2020.11.034>
52. Kocakulak, T., Arslan, T.A., Şahin, F., et al. "Determination of optimum operating parameters of MWCNT-doped ethanol fueled HCCI engine for emission reduction", *Science of The Total Environment*, 895, 165196 (2023). <https://doi.org/10.1016/j.scitotenv.2023.165196>
53. Doppalapudi, A.T., Azad, A.K., Khan, M.M.K. "Advanced strategies to reduce harmful nitrogen-oxide emissions from biodiesel fueled engine", *Renewable and Sustainable Energy Reviews*, 174, 113123 (2023). <https://doi.org/10.1016/j.rser.2022.113123>
54. Gülcan, H.E., Gültekin, N., Ciniviz, M. "The Experimental Investigation of the Effect of Methanol and Dodecanol Additives to Diesel Fuel on Engine Performance and Smoke Emissions in a CI Engine", *International Journal of Automotive Science & Technology*, 6(2) pp. 207-213 (2022). <https://doi.org/10.30939/ijastech..1074513>
55. Yesilyurt, M.K. "An Experimental Study On The Performance And Exhaust Emission Characteristics Of A CI Engine Powered By Alcohol/Biodiesel/Diesel Fuel Blends Containing Different Types Of Alcohol Isopropanol-C3, 1-Butanol-C4, And Isopentanol-C5", *Hittite Journal of Science and Engineering*, 7(2), pp. 135-148 (2020). DOI: [10.17350/HJSE19030000182](https://doi.org/10.17350/HJSE19030000182)
56. Aksoy, F., Akay, F., Baydır, Ş.A., et al. "An experimental investigation on the effects of waste olive oil biodiesel on combustion, engine performance and exhaust emissions", *International Journal of Automotive Engineering and Technologies*, 8(3), pp. 103-116 (2019). <https://doi.org/10.18245/ijaet.578227>
57. Manimaran, R., Mohanraj, T., Prabakaran, S. "Biodegradable waste-derived biodiesel as a potential green fuel: Optimization of production process and its application in diesel engine", *Industrial Crops and Products*, 192, 116078 (2023). <https://doi.org/10.1016/j.indcrop.2022.116078>

Biographies

Ayhan Uyaroglu obtained his BS in Automotive Department from the Technical Education Faculty at Gazi University, Ankara, Türkiye, in 1996. MS and PhD degrees in Graduate School Of Natural And Applied Sciences at Gazi University, Ankara, Türkiye, in 1996, 2008 and 2015, respectively. He received his BS degree in Mechanical Engineering from the Department of Mechanical Engineering at Konya Technical University, Konya, Türkiye in 2020. He is now an Assistant Professor in the Department of Motor Vehicles and Transportation Technology at Selçuk University Cihanbeyli Vocational High School, Türkiye, Konya. His research interests include Automotive Technology, Biofuels, Combustion and Emissions.

İsmet Çelikten received his BS in Higher Technical Teacher Training School at Gazi University, Ankara, Türkiye, in 1979 and MS and PhD degrees in Graduate School Of Natural And Applied Sciences at Gazi University, Ankara, Türkiye, in 1988 and 1996, respectively. He has supervised many master's and doctoral theses and taken part in various projects. He is currently an Emeritus (retired) Professor from the Department of Automotive Engineering,

Faculty of Technology at Gazi University, Türkiye, Ankara. His research expertise lies in Biofuels, Emissions and Automotive Technology.

List of Figures

Figure 1. Engine test setup

Figure 2 BSFC variations of fuels

Figure 3 Alterations of cylinder pressure and heat release rate of the test fuels

Figure 4 (a) In-cylinder gas temperature vs crank angle (b) Cumulative heat release rate vs crank angle

Figure 5 CA10 and CA50 variations against engine load

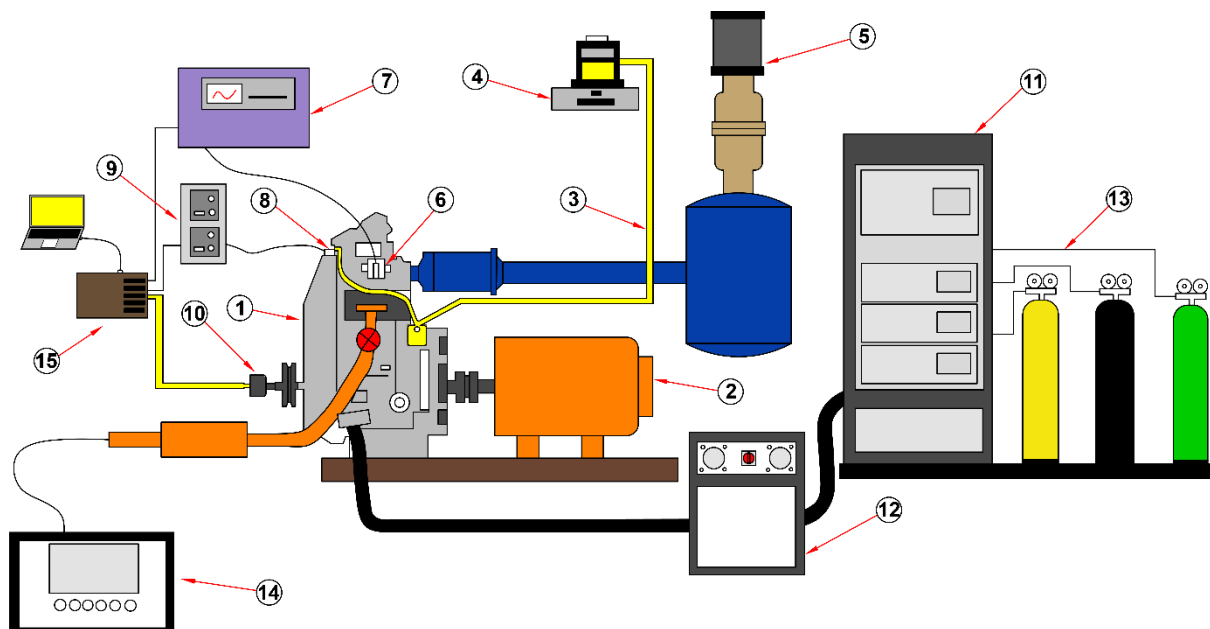
Figure 6 Combustion duration variations of the test fuels

Figure 7 RI variations of the test fuels

Figure 8 COV_{imep} and IMEP variations of the test fuels

Figure 9 CO and HC pollutants

Figure 10 NO_x and smoke pollutants



1- Single cylinder diesel test engine 2- DC dynamometer 3- Diesel fuel line 4- Sensitive scale 5- Laminar flow meter 6- In-cylinder pressure sensor 7- Combustion analyzer 8- Diesel fuel line pressure sensor 9- Diesel fuel line pressure sensor amplifier 10- Encoder 11- Emission gas analyzer 12- Emission sampling system 13- Function gases (N_2 , O_2 , H_2/He) and span gases (C_3H_8 , CO_2 , CO , O_2) 14- Emission device for smoke 15- Data acquisition card

Figure 1. Engine test setup

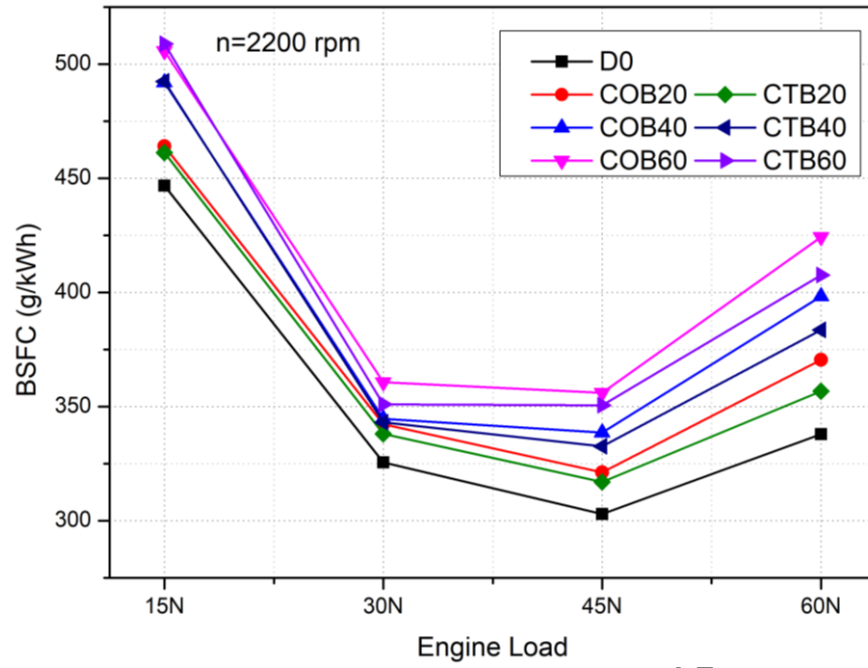


Figure 2 BSFC variations of fuels

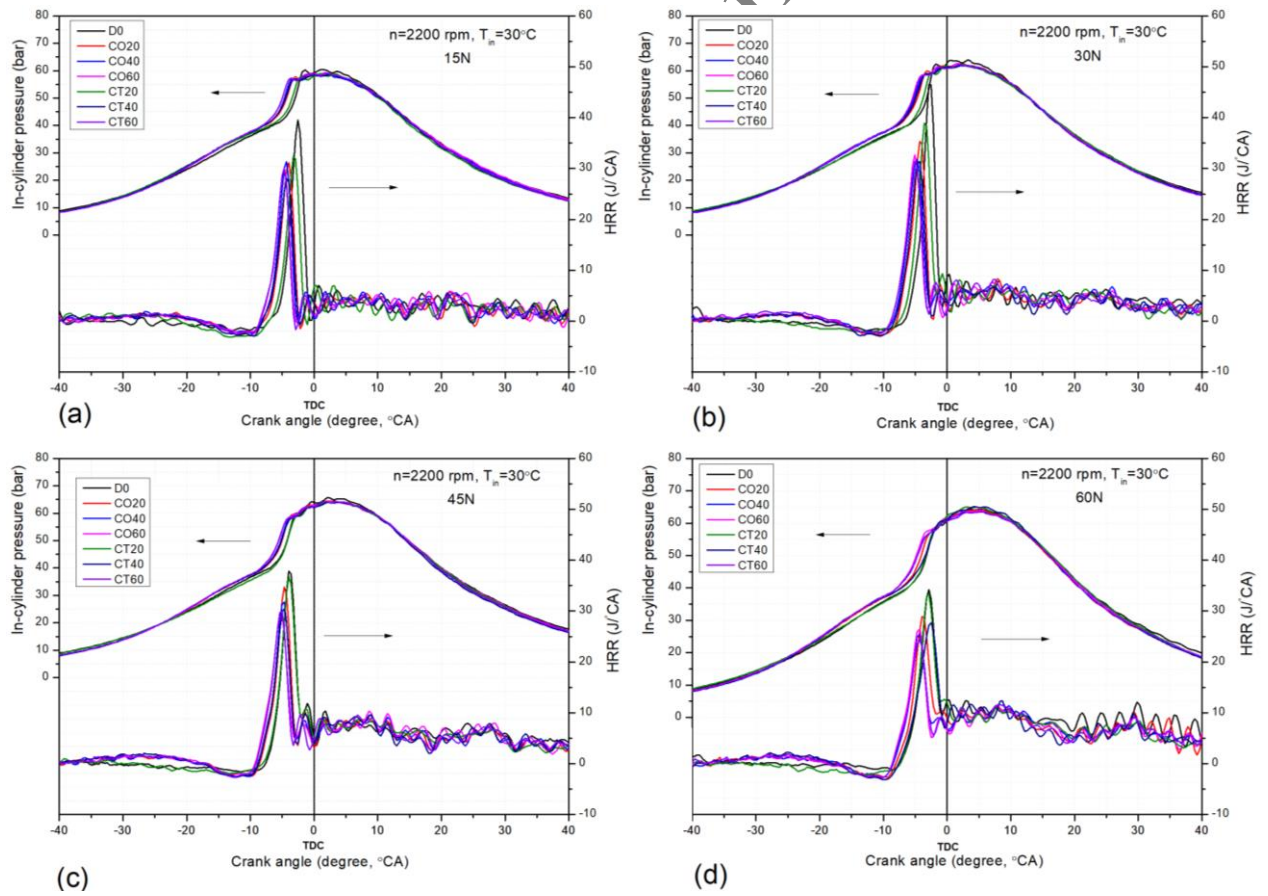


Figure 3 Alterations of cylinder pressure and heat release rate of the test fuels (a) 15N, (b) 30N, (c) 45N, (d) 60N

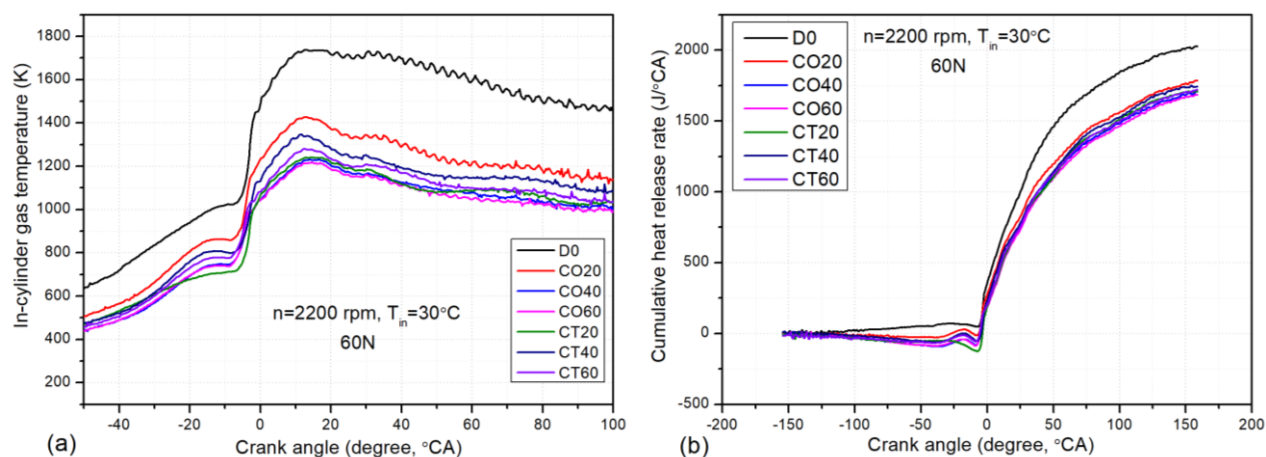


Figure 4 (a) In-cylinder gas temperature vs crank angle (b) Cumulative heat release rate vs crank angle

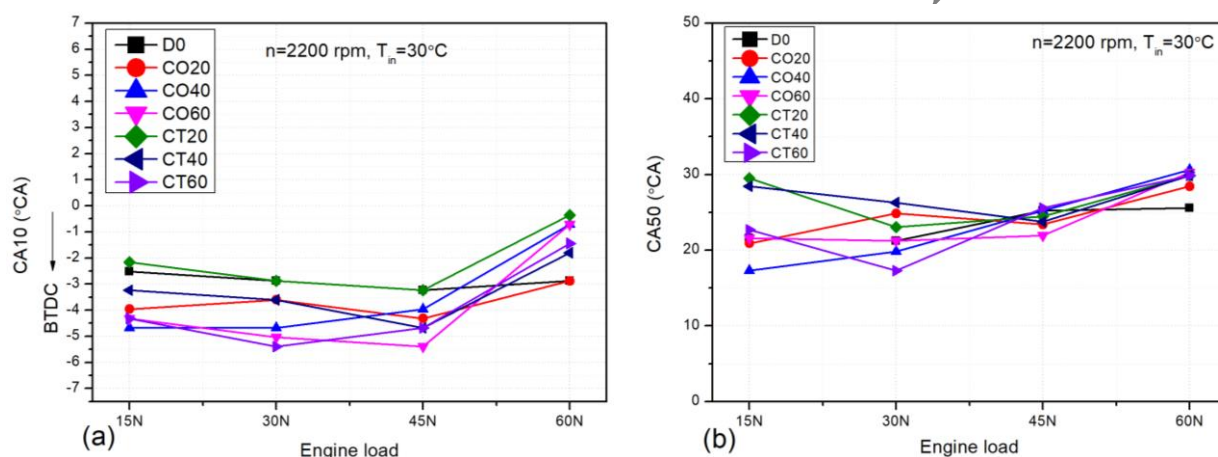


Figure 5 (a) CA10 and (b) CA50 variations against engine load

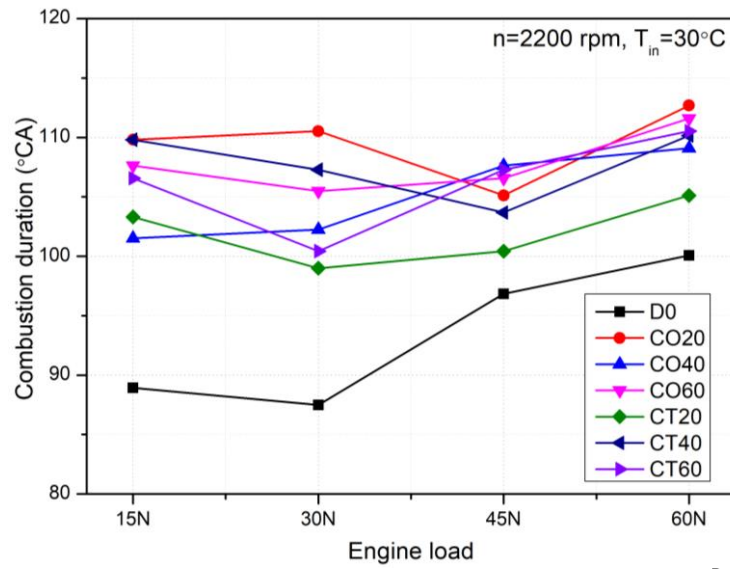


Figure 6 Combustion duration variations of the test fuels

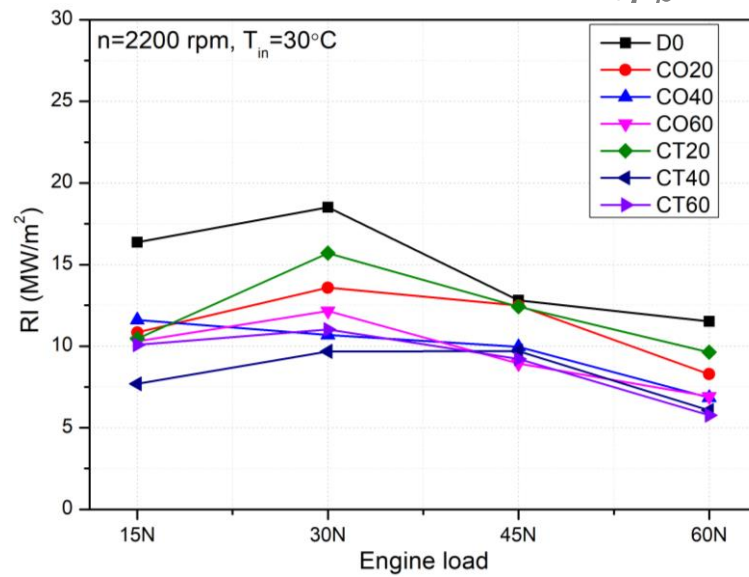


Figure 7 RI variations of the test fuels

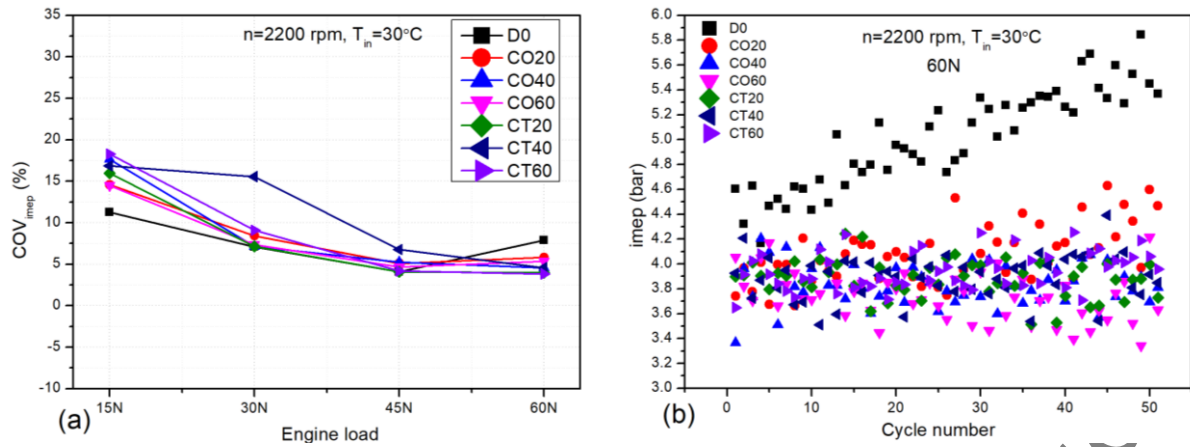


Figure 8 (a) COV_{imep} and (b) IMEP variations of the test fuels

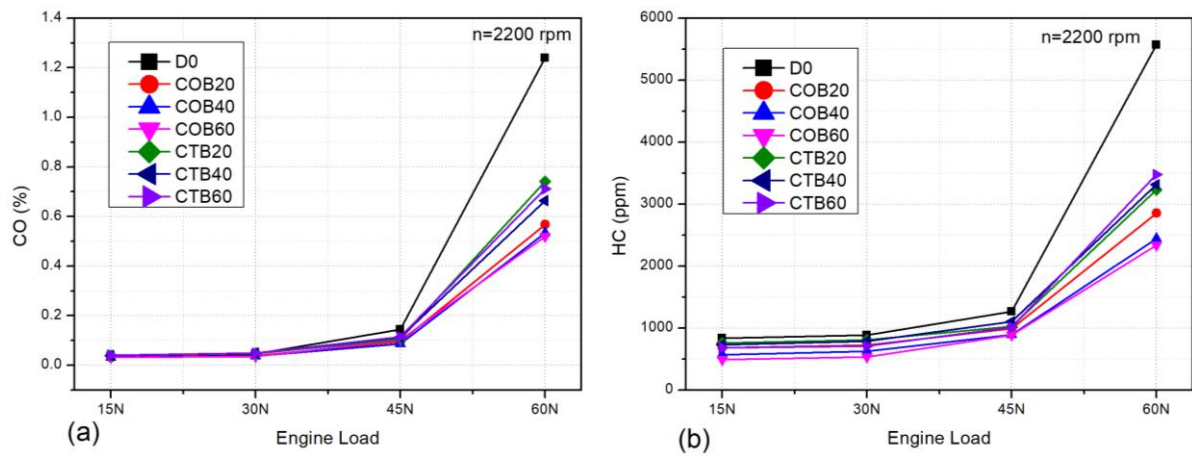


Figure 9 (a) CO and (b) HC pollutants

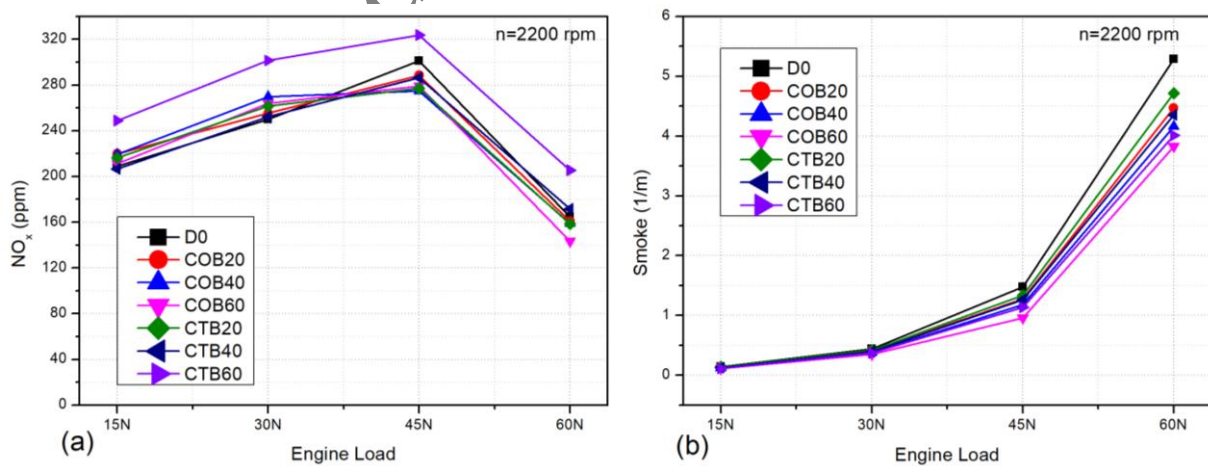


Figure 10 (a)NO_x and (b) smoke pollutants

List of Tables

Table 1 Specifications of the Antor diesel engine

Table 2 Technical specifications of devices used in emission measurements

Table 3 Specifications of pressure sensor

Table 4 The specifications of exhaust emission and measurements devices

Table 5 The properties of Crambe tataria and Crambe orientalis oils

Table 6 The properties of the test fuels

Table 1 Specifications of the Antor diesel engine

Model/Make	Antor/6LD400
Type of engine	DI-diesel engine, naturally aspirated, air cooled
Number of cylinder	1
Bore x Stroke (mm)	86 x 68
Cylinder volume (cm ³)	395
Compression ratio	18:01
Maximum power (kW)	5.4 @ 3000 rpm
Maximum torque (Nm)	19.6 @ 2200 rpm

Table 2 Technical specifications of devices used in emission measurements

Model	Graphite 52M	Topaze 32M	MIR 2M
Gases	THC	NOx	CO
Measurement procedure	HFID	HCLD	NDIR-paramagnetic
Linearity	< 1%	< 1%	< 1%
Measuring range	0-10/10000 ppm/ opt. 30000 ppm	0-10/100/1000/ 10000 ppm	0-500/10000ppm/ 50000ppm (CO)
The lowest measurement	0.05 ppm	0.1 ppm	<2% (For full scale)
Response time	<1.5	<2 s	<2 s
Device model	AVL DiSmoke 4000		
Measurement method	Partial flow Opacity	K value	
Operating range	0–100%	Accuracy 0.1%	
Accuracy (m ⁻¹)	0–99.99	0.01	

Table 3 Specifications of pressure sensor

Model	AVL 8QP500c quartz
Operating range (bar)	0-150
Measurement precision (pC/bar)	11.96
Linearity (%)	±0.6
Natural frequency (kHz)	>100

Table 4 The specifications of exhaust emission and measurements devices

	Operating range	Sensitivity	Percentage Uncertainty (%)
CO (vol %)	0-5	±0.01 vol %	0.2
THC (ppm)	0-10000	±1 ppm	0.01
NOx (ppm)	0-10000	±1 ppm	0.01
Smoke opacity (%)	0-100 %	±0.1 %	0.001
Encoder (°)	0-360	±0.36	0.1
Precision balance (g)	0-1000	±0,01	0.01
Pressure sensor (bar)	0-150	-	0.5

Table 5 The properties of Crambe tataria and Crambe orientalis oils

	C. Tataria	C. Orientalis
Refractive index (20°C)	1.4725	1.4721
FFA	0.28	0.16
Saponification number	185	187
Iodine value	100	98
Peroxide value	6.8	3.8
Density kg/m ³ (15°C)	0.916	0.916
Kinematic viscosity mm ² /s (40°C)	43.77	45.07
Fatty acids		
Myristic acid (C14:0)	0.11	0.08
Palmitic acid (C16:0)	2.76	2.68
Palmitoleic acid (C16:1)	0.23	0.17
Margaric acid (C17:0)	0.02	0.03
Heptadecenoic acid (C17:1)	0.07	0.05
Stearic acid (C18:0)	0.75	0.65
Oleic acid (C18:1)	30.13	27.34
Linoleic acid (C18:2)	16.4	12.22
Linolenic acid (C18:3)	9.15	9.38
Arachidic acid (C20:0)	0.45	0.47
Eicosenoic acid (C20:1)	1	1.18
Behenic acid (C22:0)	0.29	0.27

Erucic acid (C22:1)	37.11	44.32
Lignoceric acid (C24:0)	0.22	-
Nervonic acid (C24:1)	1.26	1.14

Table 6 The properties of the test fuels

	C. tataria	C.orientalis	D0
Density kg/m ³ (15°C)	883.1	882.7	841.75
Kinematic viscosity mm ² /s (40°C)	6.149	6.431	3.354
Flash point (°C)	181.5	181.5	74 [29]
Cold filter plugging point (°C)	13	5	-
Cetane number	57.7	58.4	53.1
Pour point (°C)	-12	-12	-
Lower heating value (MJ/kg)	40.20	40.64	42.6 [29]
Water content (mg/kg)	381.88	356.36	-